On The Development of Large Surface Vorticity in High-Resolution Supercell Simulations

Johannes M. L. Dahl[1], Matthew D. Parker[2], and Louis J. Wicker[3]
[1]*North Carolina State University, Campus Box 8208, Raleigh, NC 27695–8208, USA, jmdahl@ncsu.edu*
[2]*North Carolina State University, Campus Box 8208, Raleigh, NC 27695–8208, USA, mdparker@ncsu.edu and*
[3]*National Severe Storms Laboratory, 120 David L. Boren Blvd, Norman, OK 73072, USA, louis.wicker@noaa.gov*

I. INTRODUCTION

Tornadogenesis has been described as a three-stage process (e.g., Davies-Jones 2008a), involving i) mid-level updraft rotation, ii) development of rotation at ground level, and iii) concentration of this surface vorticity to tornadic strength. Fundamentally, the second stage is least understood and is thus the focus of the research presented in this abstract. Ultimately, this vorticity at the surface is the source of rotation in tornadoes, and without understanding this source, our knowledge about tornadogenesis and tornado maintenance will remain incomplete. One of the outstanding questions is whether baroclinic processes are required in order to accomplish rotation at the surface, or whether mere reorientation of pre-existing vortex lines is relevant. Theoretically, as well as in idealized umerical models, the latter (barotropic) effect has been shown to be capable of instigating vorticity at the surface (Markowski et al. 2003, Davies-Jones 2008b, Parker 2011). However, in full-physics simulations there are large sources of baroclinic vorticity (e.g., Rotunno and Klemp 1985, Wicker and Wilhelmson 1995, Adlerman and Droegemeier 1999). This is also supported by (pseudo-) dual Doppler analyses by Markowski et al. (2008) and Markowski et al. (2011).

This begs the question why in some situations, the barotropic mechanism seems to be relevant, while in other situations, the development of surface vorticity is dominated by baroclinic processes. Currently, it is not clear, why or in which conditions the baroclinic process dominates. The fundamental question is thus what the requirements for a downdraft are to produce either baroclinic or barotropic vorticity at the surface. Moreover, the details of the baroclinic process by which surface vorticity develops in the numerical simulations has not always been clear based on backward trajectory analyses (e.g., Wicker and Wilhelmson 1995, Noda and Niino 2010). Another open question is physical relevance of the low-level shear, which tends to be large in the environments of tornadic storms (Rasmussen and Blanchard 1998).

To tackle these questions, we ran high-resolution supercell simulations, some results of which we present in the following. In section II, we summarize the model configuration, the base-state environments used in the experiments, and briefly describe salient features of the simulations. In section III we present details about the trajectories contributing to the low-level vorticity, including important caveats involved when calculating backward trajectories, followed by section IV, where the evolution of the vorticity along forward trajectories will be described. Conclusions and ongoing work are presented in section V.

II. THE SIMULATIONS

We used the Bryan cloud model (CM1; Bryan and Fritsch 2002) version 14, which we initialized with a warm bubble in two horizontally homogeneous base-state environments. One of these environments is based on the Del City, OK, tornado from 20 May 1977. The other base state is a combination of an idealized high-CAPE thermodynamic profile and a kinematic profile that is based on the Xenia, OH, F5 tornado from 4 April 1974. This environment represents values typically associated with large tornado outbreaks in the central U.S. Although only the wind profile is inspired by the Xenia case, we will refer to this environment as "Xenia environment".

The horizontal grid spacing of the model domain is 250 m in a domain extending from 50 m AGL to 20 km AGL. The vertical grid spacing increases from about 100 m to 250 m towards the domain top. A sponge layer is used above 14 km to reduce noise due to reflecting gravity waves, and open boundary conditions are used at the lateral boundaries. A large time step of 2.5 s (2.0 s) is used for the Del City (Xenia) case. The microphysics scheme in these simulations is a Lin-type single moment scheme as implemented by Gilmore et al. 2004. To prevent egregiously chilly cold pools, the rain-intercept parameter has been reduced by a factor of eight to 10^6 m^{-4}. The simulations were run for 5400 s (90 min). The supercells in the simulation exhibit realistic features, such as a hook echo, rear-flank downdrafts, an intense, rotating updraft, as well as compact vorticity centers at the surface. Overall, the Xenia simulation exhibits larger and better pronounced features than the Del-City simulation, owing to stronger low-level gradients in the Xenia environment.

Of particular interest is the development of multiple horizontal momentum surges (HMS) in the simulations at the surface, which are flanked by sheets of vorticity, see Fig. 1. These HMSs emenate from the main downdraft that develops north of the updraft in both simulations and have also been observed in dual-Doppler analyses (see Fig. 2 in Straka et al. 2007). It is the vorticity associated with these surges that gives rise to the compact vortices at the surface.

III. TRAJECTORIES

The CM1 model has the built-in capacity to calculate forward trajectories during run time. Velocities, positions, and other fields are calculated for each parcel point using the model fields at each time step, i.e., at the time resolution of the model. This approach is the most accurate approximation possible and eliminates nearly all error associated with using lower time resolution data from the model output as in many

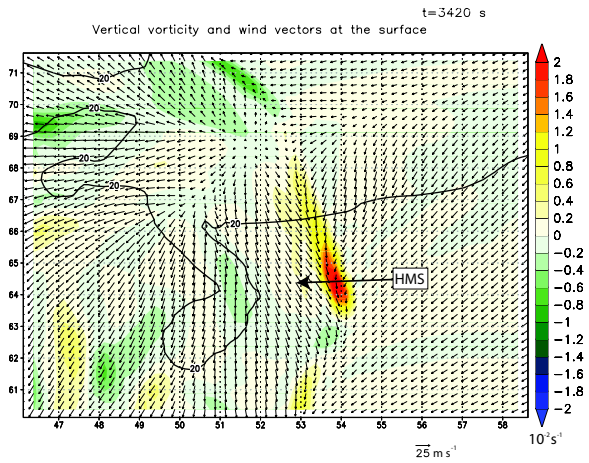

FIG. 1: Surface velocity vectors and vertical vorticity in 10^{-2} s^{-1} (see colorbar). Also, the 20 dBz reflectivity contour at 2.2 km is shown (colid black line) for orientation.

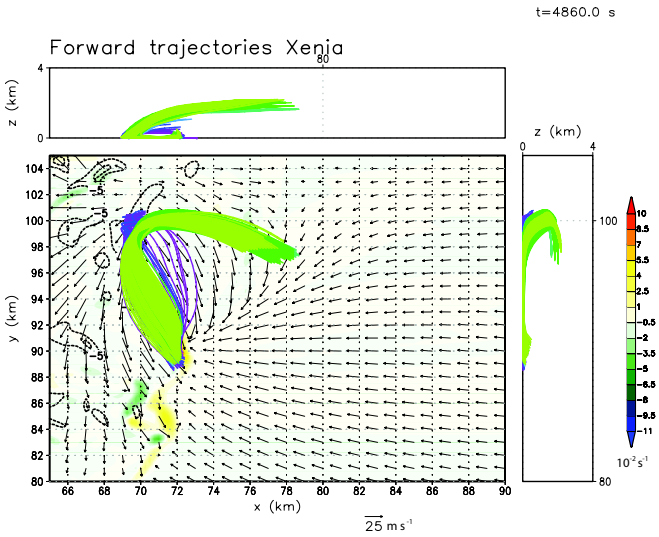

FIG. 2: Shown are the forward trajectories calculated within CM1. The trajectory colors represent the initial altitude (warmer colors correspond to higher altitudes). In addition, the horizontal storm-relative surface wind vectors are displayed, as well as the surface vorticity in 10^{-2} s^{-1} (see colorbar).

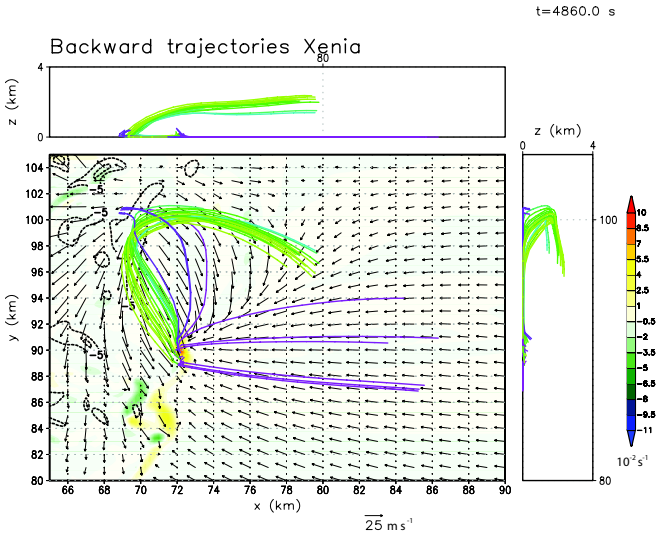

FIG. 3: Same as Fig. 2, but for the backward trajectories, calculated using 30 s history files.

previous studies. The trajectories are computationally cheap and we were thus able to release on the order of 10^6 parcels in a box centered around the storm. Minor post-processing is required to identify those parcels that end up in the area of interest. The parcels were released prior to the development of the HMS that led to an intense vorticity maximum at the surface, and only those parcels are analyzed that move along the cyclonic side of the HMS, eventually ending up in the vorticity center. The results are shown for the Xenia case in Fig. 2 (the trajectories in the Del City simulations are qualitatively identical, but are not shown here for the sake of brevity). All parcels contributing to the circulation (about 250 were identified in the Del-City case, and 850 in the Xenia case) are passing through the main downdraft, are pushed to the ground, and then become part of the circulation as they move southward via the rear flank of the storm. This result is in contradiction with numerous trajectory analyses that show an additional parcel source, i.e., the very low levels of the “inflow” sector of the storm, east of the rear-flank gustfront (e.g., Wicker and Wilhelmson 1995, Adlermann and Droegemeier 1999, Noda and Niino 2007). To understand these results, we calculated backward trajectories, using 30 s history files and a 2nd-order midpoint Runge-Kutta scheme. The velocity vector was interpolated to the parcel location trilinearly in space and linearly in time between two history files. The initial conditions were provided by the locations of the forward trajectories as they were passing through the low-level vortex. This backward integration is substantially less accurate than the online forward integration. Using this technique, we indeed reproduce the second source region of the trajectories (Fig. 3; again, similar results were obtained for the Del City simulation, which are not shown here for the sake of brevity). This suggests that the ’inflow parcels’ are likely a result of the poor temporal resolution of the history files. Given the rapid evolution of the 3D flow field prior to and during the onset of low-level rotation, it is plausible that linear interpolation within a 30 s interval may lead to inaccurate results.

IV. VORTICITY ANALYSIS

To gain insight into the vorticity evolution, we plotted the 3D vorticity vector along with the buoyant production along the forward trajectories that end up in the compact vorticity maxima at the surface, see Fig. 4. Initially, all vorticity is horizontal and streamwise. Absent baroclinic generation, this initial vorticity is “frozen” into the trajectory (e.g., Davies-Jones and Brooks 1993) and thus cannot contribute to cyclonic vorticity at the surface (e.g., Davies-Jones and Brooks 1993). However, as the parcel approaches the downdraft edge, horizontal baroclinic production contributes a *horizontal* compo-

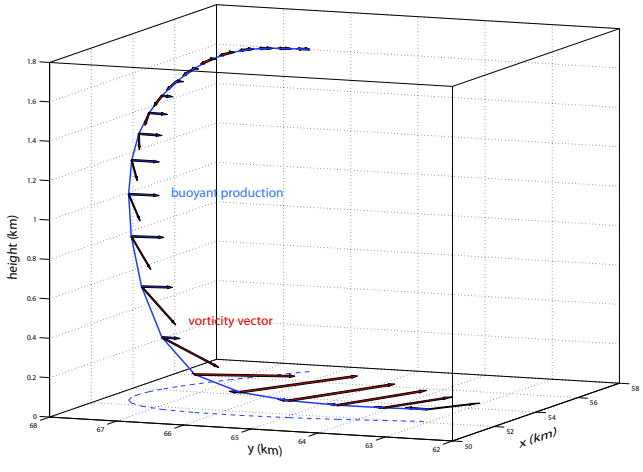

FIG. 4: 3D rendering of a trajectory as it enters the developing low-level vorticity maximum, using a forward trajectory in the Del City simulation. The blue line is the trajectory, along which the vorticity vector (red) as well as the buoyant-generation vector (blue) are plotted every 30 s. The dashed blue line is the projection of the trajectory onto the surface. The initial weak streamwise vortity is "pulled" away from the trajectory, thus allowing for a vertical vorticity component near the surface.

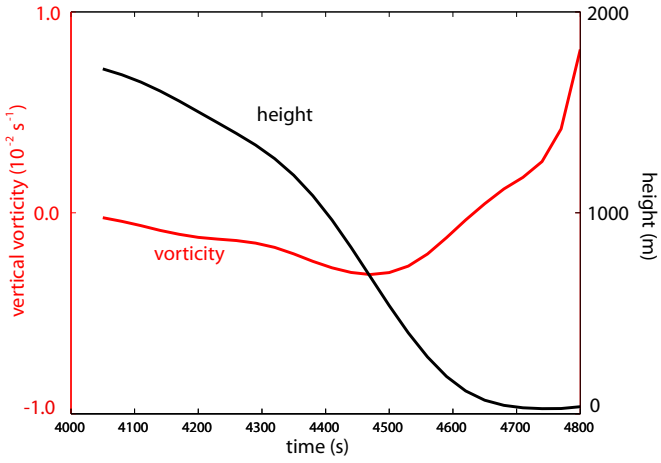

FIG. 5: Average height in meters (black line, right ordinate) and vertical vorticity in 10^{-2} s^{-1} (red line, left ordinate) as a function of time (abscissa).

nent of the vorticity vector. This baroclinic effect is a way of "freeing" the vorticity vector from being frozen into the trajectory. The result is that the vorticity now has a crosswise component. This newly-generated vorticity now behaves as though it was frozen into the fluid, but because it is no longer parallel to the trajectory, it acquires a vertical component as the trajectory bottoms out at the surface. Without this baroclinic effect, the vorticity would have remained streamwise, and consequently no vertical vorticity would result as the trajectories become horizontal at the surface. This is the process that has been proposed by Davies-Jones and Brooks (1993).

This analysis has been repeated for all identified parcels. Fig. 5 shows the average vorticity and altitude over all identified trajectories for each case. Initially, the barotropic "frozen vortex-line" effect results in negative vorticity, which is becoming more and more positive as the parcels descend (the same picture emerges in the Del City case, which is not shown here for the sake of brevity).

V. CONCLUSIONS AND ONGOING WORK

We ran two high-resolution supercell simulations using canonical base-state environments that favor tornadic supercells. Our conclusions based on this initial set of experiments are:

- Rotation at the surface is associated with horizontal momentum surges (HMS) that exhibit sheets of cyclonic and anticyclonic vorticity at their flanks. Some of these surges become favorably located beneath the low-level updraft, where the sheet of vorticity is condensed into a coherent vortex (like in Gaudet et al. 2006) and concentrated by convergence beneath the updraft. An open question is whether it is a matter of coincidence which one of the surges contributes to the vortex, or whether there are processes that single out a particular surge. Also, given the transient nature of these surges, how can a circulation longer than the time scale of an individual surge be maintained?

- All parcels in the low-level circulation are "downdraft-processed". An implication is that the low-level mesocyclone cannot "occlude" in the classic sense that it is cut off from warm air. In the simulations, it is always fed by more or less strongly rain-cooled air and never by warm environmental "inflow" air.

- Care must be taken when interpreting backward trajectories using velocity data at intervals of order 10 s. Our initial analysis suggests that the "inflow trajectories" are likely a result of the low temporal resolution of the history files, rather than physical reality. An implication is that currently used radar technology may yield insufficient temporal resolution to calculate realistic trajectories in supercell thunderstorms.

Ongoing research includes gaining more insight into the sensitivity of the backward trajectories to parameters such as the history-file interval, the accuracy of the numerical integration scheme, and the grid spacing. Moreover, the more general questions posed above, regarding the time scale of the low-level vortex vs. the time scale of individual HMSs, as well as fundamental requirements for a downdraft to produce vorticity at the surface, are being investigated.

For the latter purpose, idealized downdraft simulations are carried out in different low-level shear regimes, with initial

results suggesting this to be a promising tool to gain insight into these processes.

VI. ACKNOWLEDGMENTS

We thank George Bryan who kindly provided the CM1 source code as well as technical support. Moreover, we appreciate numerous discussions on supercell dynamics and observations with Paul Markowski, Bob Davies-Jones, Chuck Doswell, and the members of the Convective Storms Group at NCSU. Funding for this research is provided by the grant NSF ATM-0758509.

VII. REFERENCES

Adlerman E. J., Droegemeier K. K., Davies-Jones R., 1999: A numerical simulation of cyclic mesocyclogenesis. *J. Atmos. Sci.*, **56**, 2045-2069.

Bryan G. H., Fritsch J. M., 2002: A benchmark simulation for moist nonhydrostatic numerical models. *Mon. Wea. Rev.*, **130**, 2917-2928.

Davies Jones R. P., Brooks H. E. 1993: Mesocyclogenesis from a theoretical perspective. *The Tornado: Its Structure, Dynamics, Prediction, and Hazards.* 105-114.

Davies Jones R. P., 2006: Tornadogenesis in supercell storms – what we know and what we don't know. *Proc. The 86th AMS annual meeting, Atlanta, GA.*

Davies Jones R. P., 2008: Can a Descending Rain Curtain in a supercell instigate tornadogenesis barotropically? *J. Atmos. Sci.*, **65**, 2469-2497.

Gaudet B. J. and Cotton W. R., 2006: Low-Level Mesocyclonic Concentration by Nonaxisymmetric Transport. Part I: Supercell and Mesocyclone Evolution, *J. Atmos. Sci.*, **63**,1113-1133.

Gilmore M. S., Straka J. M., and Rasmussen, E. N., 2004: Precipitation and evolution sensitivity in simulated deep convective storms: Comparisons between liquid-only and simple ice and liquid phase microphysics. *Mon. Wea. Rev.* **132**, 1897-1916.

Markowski P. M., Straka J. M., and Rasmussen E. N.,2003: Tornadogenesis resulting from the transport of circulation by a downdraft: Idealized numerical simulations. *J. Atmos. Sci.*, **60**,795–823.

Markowski P. M, Richardson Y., Rasmussen E., Straka, J. M., Davies-Jones, R. P., and Trapp, R. J., 2008: Vortex lines within low-level mesocyclones obtained from pseudo-dual-Doppler radar observations. *Mon. Wea. Rev.*, **136**, 3513-3535.

Markowski P. M., Majcen M., Richardson Y., Marquis, J., and Wurman, J., 2011: Characteristics of the wind field in three nontornadic low-Level mesocyclones observed by Doppler on Wheels Radars. *Electron. J. Severe Storms Meteor.*,**6**,1-48.

Noda A. T. and Niino, H., 2010: A numerical investigation of a supercell tornado: Genesis and vorticity budget. *J. Meteor. Soc. Jap.* **88**, 135-159.

Parker M. D., 2011: Impacts of lapse rates upon low-level rotation in idealized storms. *J. Atmos. Sci.*, accepted pending minor revisions, June 2011.

Rasmussen E. N. and D. O. Blanchard, 1998: A baseline climatology of sounding-derived supercell and tornado forecast parameters. *Wea. Forecasting*, **13**, 1148-1164

Rotunno R. and Klemp J., 1985: On the Rotation and Propagation of Simulated Supercell Thunderstorms. *J. Atmos. Sci.*, **42**, 271-292.

Straka J. M., Rasmussen E. N., Davies-Jones R. P., and Markowski P. M., 2007: An observational and idealized numerical examination of low-level counter-rotating vortices toward the rear flank of supercells. *Electron. J. Severe Storms Meteor.*, **2**, 1-22.

Wicker, L. J. and Wilhelmson, R. B., 1995: Simulation and analysis of tornado development and decay within a three-dimensional supercell thunderstorm. *J. Atmos. Sci.*, **52**, 2675-2703.